ACS OMEGA

http://pubs.acs.org/journal/acsodf

Article

One-Pot Synthesis of Multiple Stimuli-Responsive Magnetic Nanomaterials Based on the Biomineralization of Elastin-like Polypeptides

Yanhong Zhou, Bo Zeng, Rui Zhou, Xialan Li, and Guangya Zhang*

Cite This: *ACS Omega* 2021, 6, 27946−27954

Read Online

ACCESS | Metrics & More | Article Recommendations | Supporting Information

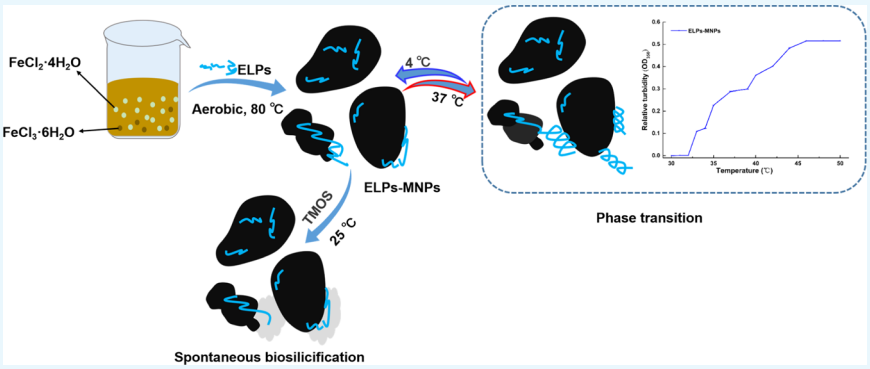

ABSTRACT: Synthesis of multiple stimuli-responsive magnetic nanomaterials in a green way remains as a big challenge currently. Herein, temperature-responsive elastin-like polypeptides (ELPs) were designed to involve in the biomimetic mineralization and successfully prepared magnetic nanoparticles (MNPs) (named ELPs-MNPs) with multiple responsiveness (temperature, magnetic, and biomimetic silicification responsiveness) in one pot. ELPs-MNPs were identified as cubic nanomaterials with an average size of about 32 nm and in line with the classic ferromagnetic behavior. Interestingly, ELPs-MNPs show clearly lower critical solution temperature phase behavior with a transition temperature of 36 °C. Moreover, ELPs-MNPs can spontaneously trigger the biosilicification of tetramethyl orthosilicate (TMOS) to entrap themselves into silicon oxide as proved by the Fourier transform infrared spectra (FTIR) and elemental mapping of transmission electron microscopy (TEM), with an average size of about 62 nm. The possible role of ELPs in the biomimetic preparation of the multiple stimuli-responsive MNPs was also addressed. The proposed novel and simple one-pot strategy to synthesize multifunctional nanomaterials with higher effectiveness is the first report for preparing MNPs with multiple stimuli response. This strategy conforms to the concept of green chemistry and will pave a new way for the design of smart biomaterials, which may have great potentials for different fields.

1. INTRODUCTION

Magnetic nanoparticles (MNPs) are new materials with great potentials, which have been developed rapidly in recent years.[1] They have been used in the fields of biomedicine, catalysis, data storage, environmental protection, and so on.[2] Recently, MNPs with multiple stimuli response are becoming particularly important in the portable, highly sensitive detection of disease markers and efficient treatment of lesions for their superior performances.[3] However, few methods are available for synthesizing them, and the common method is to couple MNPs with functional groups by chemical reagents.[4,5] For example, Krishnan *et al.* coupled the temperature-responsive poly (*N*-isopropyl-acrylamide) on the surface of MNPs and then conjugated the polymer group with the malonyl-coenzyme A synthetase (MatB) to make nanomaterials capable of responding to both temperature and magnetism.[6] Although this hybrid material achieves a dual-stimulus response, the preparation of the polymer was extremely complex and a variety of toxic organic reagents were used during the process. Therefore, researchers began to pay attention to the biomineralization of microorganisms.[7,8]

Magnetotactic bacteria could synthesize magnetite crystals with specific sizes and shapes (such as cubic octahedron, elongated hexahedron, and bullet type) in their cells under mild conditions.[9] Some proteins play an important role in the magnetite crystal biomineralization process by wrapping them in magnetosomal membranes containing these proteins.[10]

Received: July 19, 2021
Accepted: September 30, 2021
Published: October 13, 2021

https://doi.org/10.1021/acsomega.1c03821
ACS Omega 2021, 6, 27946−27954

However, most of the magnetotactic bacteria in nature are difficult to cultivate. Even after more than 30 years of exploration, few pure cultures of magnetotactic bacteria were obtained, and the output of magnetosomes is also low. Besides, the crystal size, morphology, and composition of the magnetosomes are difficult to control.[11] These disadvantages greatly hindered the large-scale application of magnetosomes. Therefore, researchers are trying to adopt the biomineralization-related proteins to prepare MNPs by biomimetic mineralization *in vitro*.[12]

The Mms protein was involved in the structural assembly of inorganic minerals in microorganisms. Artificially soluble, structurally stable Mms13cc and MmsFcc helical proteins as additives had successfully controlled the formation of MNPs in a biomineralization experiment. Magnetometry analysis indicated that MmsFcc and Mms13cc particles are pure magnetite products based on their saturation magnetization.[13] Artificially synthesized peptide M6A with the Mms6 active sequence (DIESAQSDEEVE) could react with Fe^{2+} at pH ≈ 8 to prepare MNPs with the size up to 60 nm.[14] However, both the abovementioned methods only solved the difficulties of the MNP preparation. The prepared MNPs still need to be further modified with stimuli-responsive molecules. Therefore, a green one-pot synthesis method to prepare multiple stimuli-responsive MNPs is urgently needed. To achieve this goal, we chose the stimuli-responsive elastin-like polypeptides (ELPs) to trigger ferroferric oxide biomimetic mineralization. The ELPs are derived from the hydrophobic domain of tropoelastin, a 72 kDa protein containing alternating hydrophobic and cross-linking domains. Usually, ELPs undergo a reversible phase transition in water within a narrow temperature range (called transition temperature, T_t).[15] When the solution temperature is lower than T_t, ELPs are highly soluble; when the temperature is higher than T_t, ELPs become insoluble in a coacervate phase as amorphous precipitates. The reversible phase behavior has led ELPs to self-assemble into nanoparticles (NPs) and hydrogels that are finding application in fusion protein purification, drug target delivery, and tissue engineering.[16,17] As ELPs are a class of artificial peptide polymers composed of a VPGXG pentapeptide repeat unit (where V is valine, P is proline, G is glycine, and X is a "guest residue" which can be any amino acid except proline), the functions and properties of the ELPs can be precisely manipulated by programming the X residues. ELPs have been widely studied as a protein polymer and biological material. For example, McDaniel *et al.* designed NPs with a physiologically relevant NP-aggregation transition temperature by selecting the guest residue X and molecular weight in the VPGXG repeat unit. These NPs were shown to aggregate in the vasculature of tumors that were externally heated to 42 °C, a temperature that is clinically compatible, typically in combination with external beam radiation as a treatment modality.[18]

Herein, the designed ELPs-$(K5V4F)_{40}$ with a pI of 11.28 was used to mediate biomimetic mineralization in the Fe^{2+}/Fe^{3+} precursor solution to synthesize biocompatible MNPs. They were cubic spinel structures with a size of approximately 32 nm. Interestingly, besides classic ferrimagnetic behavior, the NPs were also temperature-responsive and show reversible phase transition with a T_t of 36.0 °C. This indicated that most of the ELPs were exposed to the surface of the MNPs instead of being entrapped as ELPs could mediate the biomimetic silicification of tetramethyl orthosilicate (TMOS), which has been proved previously.[19] Therefore, the ELPs-MNP composites were also verified to trigger the spontaneous biosilicification and formed silica coats on their surface as confirmed by the elemental mappings and FTIR. Our research showed that an unprecedented biomimetic mineralization strategy named the one-pot method could directly and effectively synthesize smart biomaterials with multiple responsiveness in a green way.

This research has the following significances: First, the so-called one-pot method is a novel strategy to mediate biomimetic mineralization of MNPs, which integrated the MNP preparation and surface functionalization simultaneously. It creates a green and safe way for synthesis of multifunctional biomaterials, which provides a new idea for subsequent researchers to prepare smart materials. Second, the one-pot method is milder under reaction conditions and more costly and time saving, which conforms to the concept of sustainable development. Finally, ELPs are programmable with excellent biocompatibility, and it will pave a new way for the design of functional nano-biomaterials with great application potentials for biomedical field.

2. EXPERIMENTAL SECTION

2.1. Materials. All reagents in this study were of analytical grade and purchased from Sigma-Aldrich. *E. coli* strains BL21 (DE3), plasmid pUC-19-ELPs40, and pET-22b(+) were preserved in our laboratory.

2.2. Construction of ELPs-$(K5V4F)_{40}$. ELPs-$(K5V4F)_{40}$ (the accession number of the coding gene in NCBI is MZ073641) with 40 repeats of VPGXG ("X" was a combination of lysine/valine/phenylalanine = 5:4:1) was designed with a tryptophan at the C-terminus to determine their concentration by UV spectrophotometry. The expression plasmid of ELPs-$(K5V4F)_{40}$ is shown in Figure S1, and the gene and protein sequences are shown in the Supporting Information.

2.3. Expression and Purification of ELPs-$(K5V4F)_{40}$. The plasmid tailoring the coding gene of ELPs-$(K5V4F)_{40}$ was transformed and overexpressed in the *E. coli* strain BL21 (DE3). The strain was incubated at 37 °C for 12 h in Luria–Bertani (LB) supplemented with 100 μg mL^{-1} ampicillin. Then, the abovementioned activated cells were incubated at 37 °C in terrific broth (TB) supplemented with 100 μg mL^{-1} ampicillin until the value of OD_{600} was between 0.4 and 0.6. Isopropyl-β-thiogalactoside (IPTG) was added to a final concentration of 0.5 mmol L^{-1} for inducing at 20 °C for 20 h. Cells were collected by centrifugation at 4000*g* for 20 min. After discarding the supernatant, the harvested cells were resuspended in PBS (pH 7.0) at 4 °C. Then, the cells were ultrasonically disrupted in an ice bath. To harvest the crude protein, the insoluble cell debris was removed by centrifuging at 4 °C (12,000*g*, 20 min).

The ELPs were purified by the inverse transition cycling (ITC) method, the same as our previous study.[20] The purified ELPs were dissolved in PBS buffer (pH 7.0) and stored at −20 °C. The purity of ELPs-$(K5V4F)_{40}$ was evaluated with the sodium dodecyl sulfate polyacrylamide gel electrophoresis (SDS-PAGE). Moreover, the concentration was determined by UV spectrophotometry (Analytik Jena AG, Jena, Germany).

2.4. Biomimetic Mineralization of Magnetite. To prepare 70 ml of reaction mixtures, 20 ml of ELPs with the magnetite precursor ($FeCl_3{\cdot}6H_2O$ and $FeCl_2{\cdot}4H_2O$) was mixed with 50 ml of the alkaline sodium hydroxide solution prepared with double-distilled water. The final concentration

https://doi.org/10.1021/acsomega.1c03821
ACS Omega 2021, 6, 27946−27954

of $FeCl_2$, $FeCl_3$, and NaOH was 0.31, 0.09, and 2.57 mol L^{-1}, respectively. The concentrations of ELPs-$(K5V4F)_{40}$ were 0.02, 0.04, 0.1, and 0.15 mmol L^{-1}. The reaction mixture was stirred at 80 °C for 108 min at a rate of 1000 r min^{-1} (IKA-C-MAG HS 7). The same experiment without ELPs was set as the control.

After biomimetic mineralization, magnetite was magnetically separated and washed three times with ddH_2O. The concentration of ELPs in the supernatant was determined by UV spectrophotometry at 280 nm. The binding efficiency of ELPs-$(K5V4F)_{40}$ with MNPs was calculated as follows

$$\eta = \frac{A - B}{A} \times 100\%$$

where A is the total concentration of ELPs-$(K5V4F)_{40}$ and B is the concentration of ELPs-$(K5V4F)_{40}$ in the supernatant after magnetic separation.

2.5. Temperature Responsiveness of the Biomimetic MNPs. To measure the responsiveness of the ELPs-MNPs to temperature, a total volume of 1 mL of PBS solution of ELPs-MNPs (pH 7.0, final concentrations: NaCl: 2.5 mol L^{-1}, and ELPs-MNPs: 0.05 g) was measured at OD_{350} nm by UV spectrophotometry, and the sample was heated within the range of 25−50 °C. In addition, this sample was incubated at 37 and 0 °C for obtaining the dynamic change diagrams before, during, and after the ELP phase transition.

2.6. Spontaneous Biosilicification of the ELPs-MNPs. To prepare the stock solution of MNPs, 0.1 g of ELPs-MNPs was accurately weighed and suspended in a PBS (pH 7.0) buffer with ultrasound. Silicic acid was prepared with TMOS in 1 mmol L^{-1} hydrochloric acid (pH 3.5) to a final concentration of 1 mmol L^{-1}. The ELPs-MNPs were mixed with the TMOS-HCl solution at the V/V ratio of $V_{ELPs\text{-}MNPs}/V_{TMOS\text{-}HCl}$ = 9: 1. The mixture was allowed to stand for 5 min at room temperature to obtain the precipitate, which was dried overnight at 50 °C as previously described.[21]

2.7. Characterizations of the ELPs-MNPs. TEM and mapping TEM of the magnetite were performed with TEM FEI Talos F200X (ThermoFisher Scientific, USA) operated at 200 KV. The TEM images were analyzed with the software of ImageJ 1.47. Thermogravimetric analysis (TGA) was performed on a Netzsch TG 209 F3 analyzer (Germany). Measurements were carried out over a temperature range of 25−900 °C at a constant heating rate of 10 °C min^{-1} under nitrogen. Powder X-ray diffraction (XRD) measurements were performed on an X'Pert Pro MPD (Holland) with the CuKα radiation, with the scan range set from 5 to 80° in 2θ (5° min^{-1}) with X'Pert HighScore Plus software. Hysteresis cycles of the sample were run using a vibrating sample magnetometer (VSM, LakeShore-7404, USA) at 298.15 K. FTIR analyses were recorded at room temperature in the transmission mode using a Perkin Elmer spectrometer 65 FTIR instrument (Waltham, MA, USA).

3. RESULTS AND DISCUSSION

3.1. Protein Purification. SDS-PAGE electrophoresis gel of the ELPs-$(K5V4F)_{40}$ purified by two-round ITC showed an intense band of about 20 kDa (see Figure 1), which was slightly larger than the theoretical molecular weight 17.45 kDa. This may be due to the special structure of the ELPs which was usually observed in previous reports.[22] The purity of ELPs was confirmed to be higher than 95% according to the Tanon Gis-2008, which can be used for the later experiments.

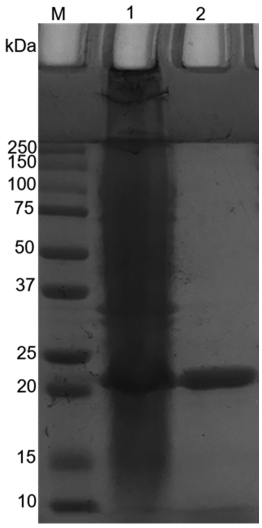

Figure 1. SDS-PAGE of ELPs-$(K5V4F)_{40}$. M: protein molecular weight maker; lane 1: the lysates; and lane 2: the purified ELPs$(K5V4F)_{40}$ after two round ITC.

3.2. Characterization of the Biomimetic Magnetite and the Binding Efficiency Optimization. XRD data (Figure S2) of the washed precipitates displayed the characteristic peaks of MNPs at 2θ = 30.18, 35.53, 43.30, 53.99, 57.21, and 62.68° corresponding to the (220), (311), (400), (422), (511), and (440) crystal planes of Fe_3O_4, respectively. These results indicated that NPs obtained from the biomimetic mineralization experiments were mainly magnetite regardless of the presence of ELPs-$(K5V4F)_{40}$, matched well with those of the Fe_3O_4 (JCPDS card. no. 79-0418).[23] The narrow sharp peaks of these samples indicated that the NPs had relatively high crystallinity.[24] TEM of the abovementioned samples (Figure 2a,c) showed a cubic spinel crystal structure in morphology. The average size of the ELPs-MNPs (32 ± 12 nm) (Figure 2b) was slightly larger than that of the control (9 ± 8 nm, which is consistent with the previous report) (Figure 2d) without the ELP additive.[25] This result indicated that the ELPs-$(K5V4F)_{40}$ could increase the NP size. Similar results were also observed previously. For example, the MNP biomineralization in the presence of the magnetosome membrane protein MamC showed the elongation of these crystals in one [111] direction due to the approximate distance between Glu66-Asp70 and the Fe cations in (111), (311), and (110) planes creating a template effect.[26] The elemental mappings of C and N in the TEM image (Figure 2e) of ELPs-MNPs were evidence that there existed some ELPs in the biomimetic MNPs.

To determine the stability and possible composition of MNPs-control and ELPs-MNPs, their TGA analysis was carried out. As shown in Figure 3a, MNPs-control exhibited a first weight loss of 2.55% below 220 °C mainly due to the dehydration and evaporation of little residual solvent. This was followed by a second weight loss of 2.27%, which can be attributed to physically absorb organic compound residues left in the synthesis processes. For the ELPs-MNPs, the first dehydration weight losses approached 2.74% below 220 °C. A second weight loss of 3.34% for ELPs-MNPs when the temperature was heated from 220 to 367 °C indicated that ELPs were immobilized in the biomimetic MNPs with a content of 1.07% (w/w).[27] FTIR analysis (Figure 7c) also

https://doi.org/10.1021/acsomega.1c03821
ACS Omega 2021, 6, 27946−27954

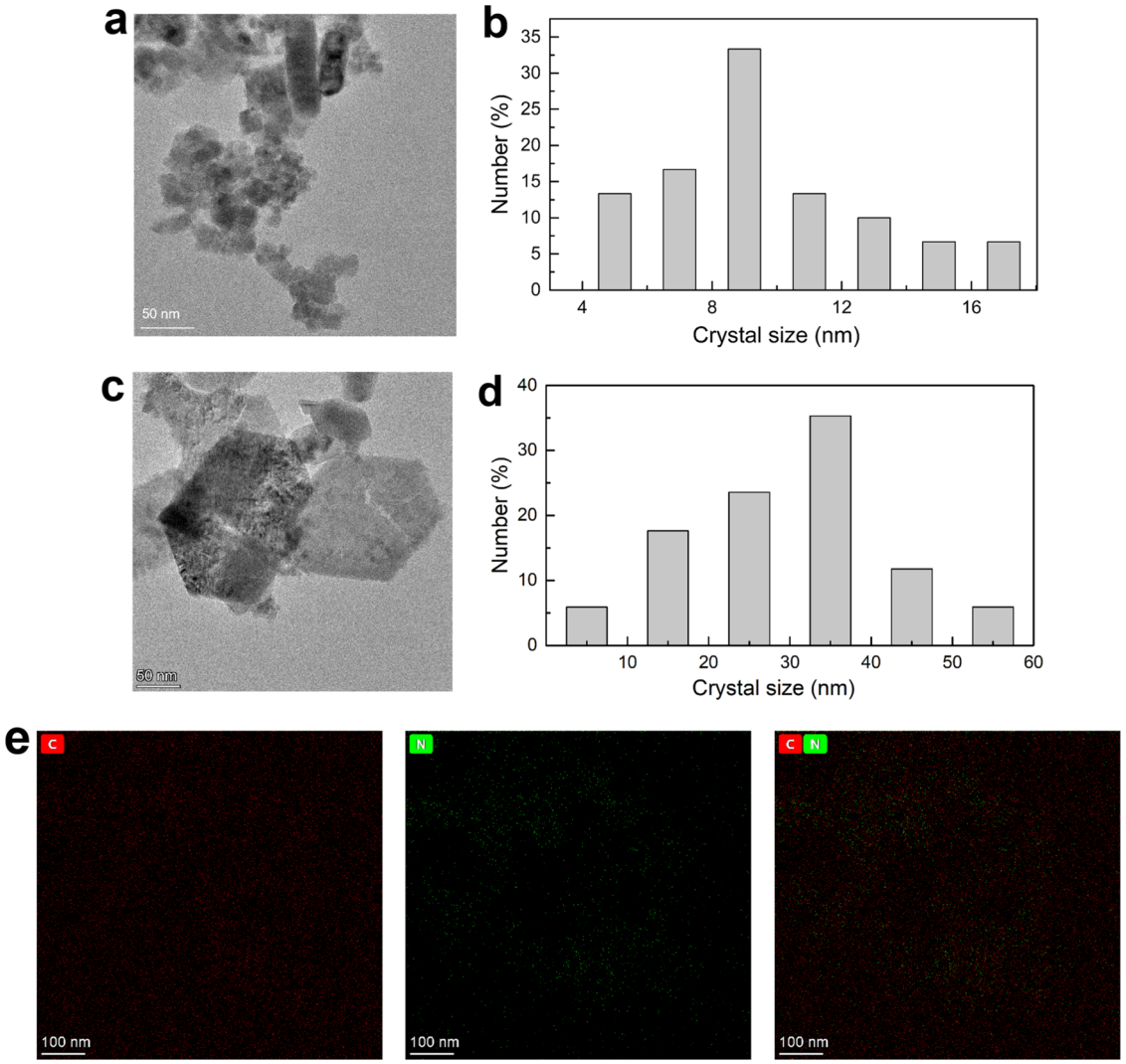

Figure 2. (a,b) TEM image and size distribution of MNPs-control. The scale bar corresponds to 50 nm. (c,d) TEM image and size distribution of ELPs-MNPs. The scale bar corresponds to 50 nm. (e) Elemental mappings of C and N in the TEM image of ELPs-MNPs. The scale bar corresponds to 100 nm.

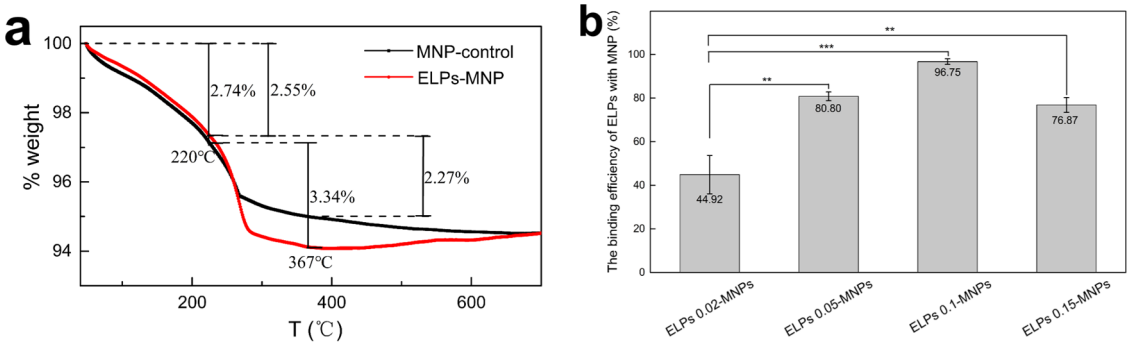

Figure 3. (a) TGA data of MNPs-control and ELPs-MNPs. (b) Influences of ELPs-$(K5V4F)_{40}$ concentration on MNPs. Mean ± SD, $n = 3$. ** indicates $p < 0.01$, and *** indicates $p < 0.001$.

showed the N−H_2 part single-bond stretching vibration peak at 1130 cm^{-1}, the C−H trans deformation vibration absorption peak at 900 cm^{-1}, and the −CH_2− long carbon chain-saturated hydrocarbon stretching vibration absorption peak at 790 cm^{-1}, which further confirmed that the samples contained a protein component to form ELPs-MNPs.[28] The abovementioned results indicated that the ELPs-$(K5V4F)_{40}$ could bind with the crystals during the biomimetic mineralization process.

To ensure more ELPs-$(K5V4F)_{40}$ bound to the MNPs, we optimized the binding efficiency of ELPs with MNPs by changing the ELP concentrations during the process of biomimetic mineralization of magnetite. The binding efficiency enhanced with the improvement of the ELP concentration,

https://doi.org/10.1021/acsomega.1c03821
ACS Omega 2021, 6, 27946−27954

which increases from 44.92 to 80.8 and 96.75% when the concentration of ELPs increase from 0.02 to 0.05 and 0.1 mol L^{-1}, respectively (Figure 3b).

However, the binding efficiency was decreased to 76.87% when the concentration of ELPs was 0.15 mol L^{-1}. The differences between them are extremely significant with the p value less than 0.01 ($p < 0.01$). As the least loss of ELPs-$(K5V4F)_{40}$ was only ~3.25%, which is good enough for preparing the biomimetic magnetite, we chose a concentration of 0.1 mol L^{-1} to prepare ELPs-MNPs (named ELPs-0.1 MNPs) for later experiments. In addition, the ELP leakages of the biomimetic magnetite in several commonly used solutions (such as dd H_2O, Tris-HCl, and PBS buffer) were assayed by detecting the concentration of ELPs in the supernatant after incubating the magnetite in the solutions for 120 h. To our surprise, almost no detectable ELPs-$(K5V4F)_{40}$ was observed in the supernatant after magnetic separation, indicating that ELPs were tightly bound with the magnetite without leakage.

To further explore the binding mode of ELPs-$(K5V4F)_{40}$ and the biomimetic MNPs, 0.1 g of ELPs-MNPs was incubated for 1 h in 50 mmol L^{-1} PBS buffer (with the pH values of 5.5, 7.0, and 8.5) and different ionic strength (by adding NaCl with the final concentration of 0.5, 1.0, and 5.0 mol L^{-1}) according to previous study,[29,30] and the results are shown in Table 1.

Table 1. Elution of ELPs-MNPs

conditions of elution (pH/NaCl concentration, mol L^{-1})	eluted ELPs, %
5.5/5.0	0
8.5/5.0	8.29 ± 0.05
7.0/5.0	7.02 ± 0.10
7.0/0.5	8.34 ± 0.01
7.0/1.0	6.57 ± 0.36
7.0/1.0; +0.5% (w/v) Tween 20	12.29 ± 0.05
7.0/5.0; +0.5% (w/v) Tween 20	16.40 ± 0.30

The first five results indicated that the abovementioned eluent could remove very few ELPs-$(K5V4F)_{40}$ bound on the NPs whether changes in pH, increases in the concentration of sodium chloride or more acidic in the reaction system. The nonionic detergent Tween 20 was therefore used to examine the possible role of hydrophobic interactions between the ELPs and the biomimetic MNPs. The result showed that approximately 12.29 and 16.40% of ELPs were eluted in the presence of 0.5% Tween 20 at different concentrations of NaCl, indicating that very few ELP molecules were bound by the hydrophobic interaction. Therefore, we could conclude that the binding of ELPs-$(K5V4F)_{40}$ with MNPs was not mainly driven by electrostatic and hydrophobic interactions.

In fact, hysteresis cycles of the MNPs-control and ELPs-MNPs (Figure 4) showed that the remnant magnetization and magnetic coercivity decrease with the ELPs-$(K5V4F)_{40}$ participating.

These crystals still conformed to the classic ferrimagnetic behavior, which was also consistent with some previous studies.[30,31] For example, the later crystal hysteresis loop in both MNPs-control and that in the presence of high content glutamic acid (or lysines) showed superparamagnetic behavior (no magnetic hysteresis).[32,33]

About biomimetic mineralization mediated by single amino acid, the interaction between the amino acid and minerals during nucleation and growth not only changed the size in morphology but also varied the magnetism from ferrimagnetic

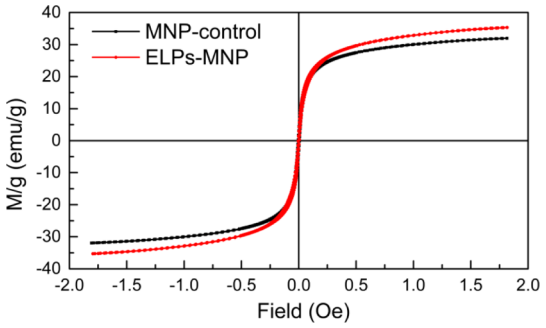

Figure 4. Hysteresis cycles of the MNPs-control and ELPs-MNPs.

behavior to superparamagnetic behavior of particles. Amino acids were usually fixed on the crystal surface because the dispersibility increased in aqueous medium.[32] However, ELPs-$(K5V4F)_{40}$ with random coil in the soluble state was obviously different from the single amino acid. According to the abovementioned results, we speculated that ELPs-$(K5V4F)_{40}$ participated in the process of nucleation and crystallization, rather than simply interacting with the surface of the crystal. The side chains of residues of Lys in the ELPs-$(K5V4F)_{40}$ may play an important role, and as we all know, the lysine (pI = 9.74) has a long side chain and the amino group at the end of the side chain provides a positive charge. Besides, the amino group is hydrophilic, while the hydrocarbon chain is hydrophobic. Moreover, there were 20 lysine residues in each of the ELPs-$(K5V4F)_{40}$.

3.3. Unique Phase Transition Phenomenon of the Biomimetic Magnetite. As over 96.75% of the ELPs were tightly bound to the biomimetic magnetite without leakage and the ELPs were thermoresponsive smart peptides, we wondered if the prepared biomimetic magnetite was also sensitive to the temperature. To confirm the speculation, the phase transition curves at 350 nm of the pure ELPs-$(K5V4F)_{40}$, MNPs-control, and ELPs-MNPs in PBS solutions were measured. The phase transition of ELPs could be divided into three stages. (1) When the temperature was lower than T_t of ELPs, the OD_{350} nm was constant (near to zero) and the ELPs were highly soluble; (2) when the temperature of the solution was higher than T_t, the values of OD_{350} nm increased sharply in the narrow temperature range (within 5 °C) as the ELPs aggregated in the solution. (3) When the temperature was continuously increased (>T_t), the values of OD_{350} nm remained unchanged. Similarly, the ELPs-MNPs also showed the three stages clearly, although the temperature range was much wider (about 14.0 °C) in the second stage. The T_t value of ELPs-$(K5V4F)_{40}$ was 29.7 °C, while the T_t value of ELPs-MNPs was 36.0 °C. This phenomenon may have a reason: some ELPs were exposed on the surface of ELPs-MNPs and some ELPs were still wrapped in the crystal; thus, their response to temperature was not so sensitive as the purified ELPs-$(K5V4F)_{40}$. In contrast, the value of OD_{350} of the MNPs-control remained stable near zero, which indicated that the magnetite itself could not respond to temperature at all (Figure 5).

To show the results more vividly, a video (see Supporting Information) and some screenshots (Figure 6a) were taken. As can be clearly seen, ELPs-MNPs in the PBS solution undergo a phase change immediately at 37 °C, they form aggregates that are visible to the naked eyes (the first photograph in Figure 6a), then the particles moved to the direction of the magnet at

https://doi.org/10.1021/acsomega.1c03821
ACS Omega 2021, 6, 27946−27954

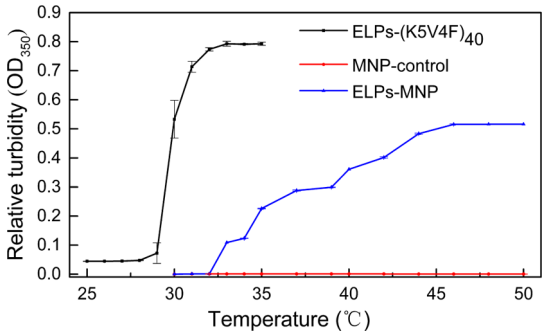

Figure 5. Phase transition temperatures of ELPs-$(K5V4F)_{40}$, MNPs-control, and ELPs-MNPs.

37 °C (the second photo in Figure 6a), the solution became clear until the particles were all magnetically separated (the third photo in Figure 6a), these results indicated that ELPs-MNPs could run phase transition when heated to the T_t, and the phase transition was reversible when the temperature decreases to 4 °C (the last photograph in Figure 6a).

As a comparison, the phase transition of the pure ELPs-$(K5V4F)_{40}$ is also presented in Figure 6b. As can be seen, typical phase transition phenomena occurred. However, when they were in the magnetic field, no aggregates moved to the direction of the magnet (the second and third photographs in Figure 6b). Moreover, two videos (see the Supporting Information) also showed the change from turbidity to clear in the phase transition process of ELPs-MNPs and ELPs-$(K5V4F)_{40}$, but the MNPs-control did not. In short, ELPs-MNPs had the advantage of being responsive to temperature.

Based on the abovementioned results, we believe that ELPs-$(K5V4F)_{40}$ participated in the crystal nucleation process by forming coordination bonds with the N atom of the amino group in the side chain of lysine with the precursor Fe^{2+} in biomimetic mineralization and then gradually nucleated and grew. During the process, some ELPs-$(K5V4F)_{40}$ were wrapped inside the crystal, but there were still some ELP molecules exposed on the surface.

3.4. Biosilicification of the Biomimetic Magnetite. As mentioned above, some ELPs are exposed on the surface of the biomimetic magnetite, yet they tightly are bound to them. Besides, ELPs have been proved to mediate the spontaneous biomimetic silicification of TMOS.[19] Therefore, we speculated that the ELPs-magnetite composites might also have this advantage, thus endowing the material a new function of self-biosilicification. As shown in Figure 7a, the resulted solids showed the irregular cubic spinel in the morphology after the spontaneous silicification experiment. The elemental mappings of C, N, and Si in the TEM image further proved that the shell was silica, and ELPs also existed in the biomimetic MNPs. The average size is 62 ± 17 nm (Figure 7b), which is bigger than the original magnetite (32 ± 12 nm), indicating that the ELPs-MNPs might be coated with a shell. At the same time, FTIR analysis (Figure 7c) of the abovementioned samples showed that the Si−O−Si antisymmetric stretching vibration absorption peaked at 1080 cm^{-1} and the Si−OH stretching vibration absorption peaked at 980 cm^{-1}, which fully confirmed that the samples contained a silica component to form SiO_2@ELPs-MNPs. The abovementioned results indicated that the ferroferric oxide MNPs prepared by ELPs-$(K5V4F)_{40}$ in the biomimetic mineralization could further mediate spontaneous biosilicification without other chemical modification under a mild condition. There might be some significances of the spontaneous biosilicification of the ELPs-MNPs. First of all, it greatly reduces the risk of iron being oxidized, thereby retaining strong magnetism for a long time. Second, the formation of the silica coating is easier for functionalizing the surface, which is conducive to the immobilization of enzymes, making it an ideal carrier through introducing various catalytically active substances.[34,35]

4. CONCLUSIONS

In summary, we proposed a novel "all-in-one" strategy to prepare the multiple stimuli-responsive magnetic nanomaterials by means of the biomimetic mineralization of ELPs-$(K5V4F)_{40}$ to fine-tune the nanomaterials in morphology and size. Compared with the previous methods,[36] this one-pot method was simpler in operation and did not require oxygen

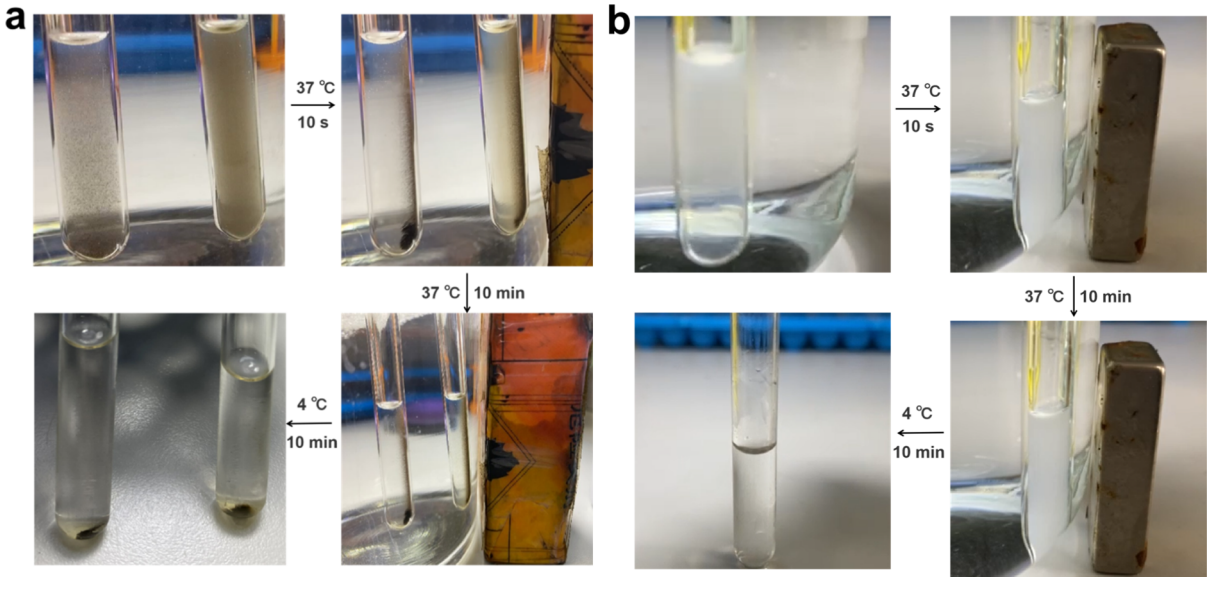

Figure 6. (a) Phase transition of ELPs-MNPs (right) and MNPs-control (left). (b) Phase transition of ELPs-$(K5V4F)_{40}$.

https://doi.org/10.1021/acsomega.1c03821
ACS Omega 2021, 6, 27946−27954

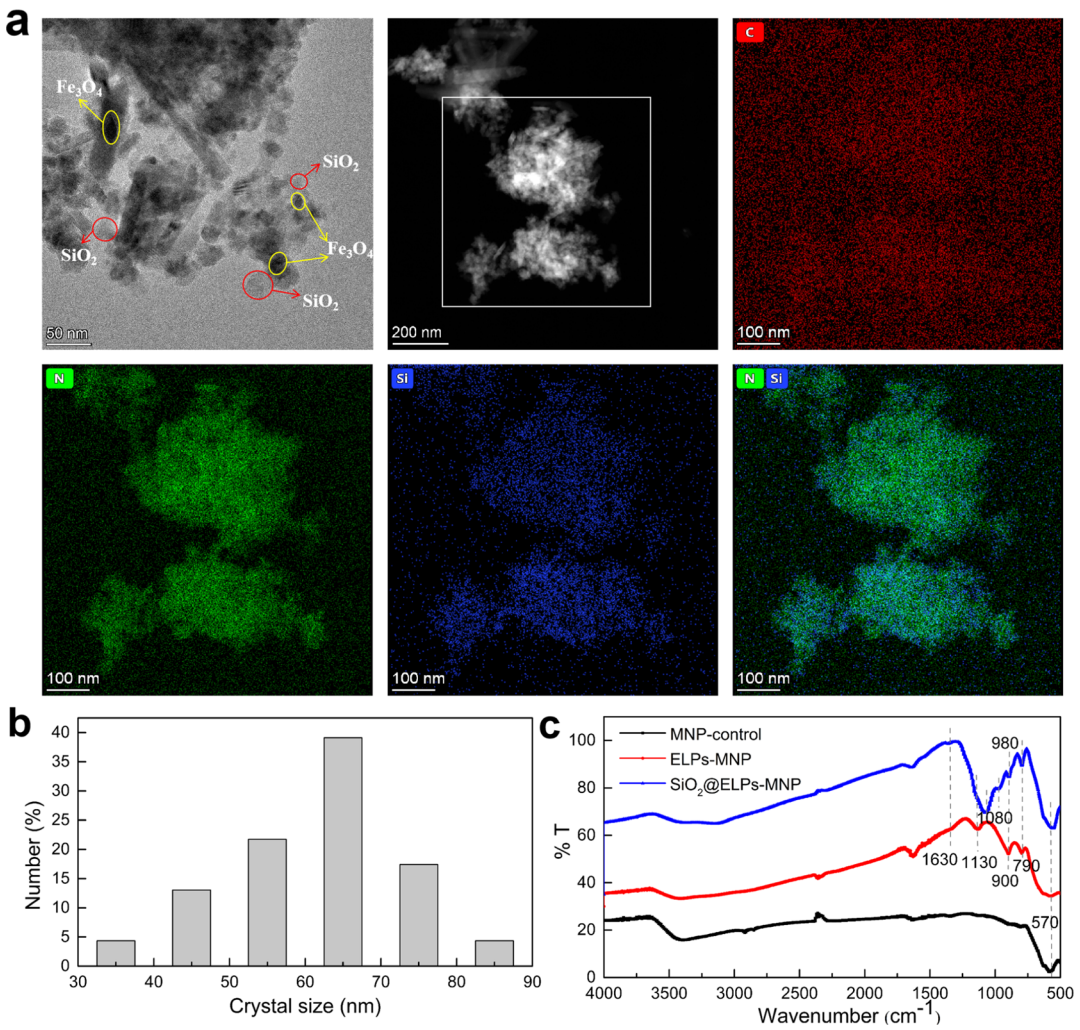

Figure 7. (a) TEM image. The scale bar corresponds to 50 nm or 200 nm. The elemental mappings of C, N, and Si in the TEM image of SiO_2@ELPs-MNPs. The scale bar corresponds to 100 nm. (b) Size distribution of SiO_2@ELPs-MNPs. (c) FTIR spectra of MNPs-control, ELPs-MNPs, and SiO_2@ELPs-MNPs.

isolation, milder and faster in reaction, and less harmful to the environment and operators, which is consistent with the idea of green chemistry in preparing multifunctional MNPs. The one-pot method breaks the limitations of traditional chemical preparation and modification of materials and paves a new way for the synthesis of polypeptide-MNP composites. Besides the response to magnets in a magnetic field with classic ferrimagnetic behavior, the resulted biomimetic magnetite also showed a unique reversible phase transition behavior in the temperature range of 32−46 °C. Encouragingly, the ELPs-MNPs could spontaneously form protective layers of silica on their surfaces by means of biosilicification, which provided a safety guarantee for the potential biomedical application of bio-nanomaterials.

The inherent mechanism of this highly advantageous one-pot method for green synthesis of the multifunctional nanomaterials based on ELPs was different from the single amino acid or the proteins related to biomineralization involved in previous studies. In an alkaline solution, the nitrogen atoms in the amino groups of ELPs-$(K5V4F)_{40}$ side chain stabilized the tight bond between ELPs and nanomaterials through coordination with the iron cation and participated in the formation of crystal nuclei. By this way, the ELPs tightly bound inside the crystal instead of only interacting with the crystal surface.

As ELPs-$(K5V4F)_{40}$ was in random a coil structure in the soluble state, it allows them to remain stable under the alkaline conditions at 80 °C during the preparation of the biomimetic magnetite. However, most of the natural proteins are unstable and tend to be denatured under this harsh condition. Perhaps, further research studies would concern more mild reaction conditions (*e.g.*, lower temperature) to keep the original structure of biological molecules. Excitingly, we have made preliminary achievements in exploring milder biomimetic mineralization conditions. Functionalized MNPs were successfully prepared by biomimetic mineralization using elastin-like polypeptide and a native protein SpyCatcher at 30 °C and used for enzyme immobilization. This would maximize the activity of biological macromolecules and expand the application field of multifunctional materials in various disciplines. Therefore, we believe that this study is meaningful and expected to inspire more interest in the development of functionalized MNPs that are applied as biomimetic materials and shows potential biomedical application of bio-nanomaterials. A smaller size of MNPs compared with microparticles and generally better controlled release properties than liposomes may improve patient acceptance and compliance. Considering the low cost,

https://doi.org/10.1021/acsomega.1c03821
ACS Omega 2021, 6, 27946−27954

abundance, ease of purification, and wide acceptance in the unique binding properties, the biomimetic magnetites are prospected to be promising candidates for tumor-targeted drug delivery.

■ ASSOCIATED CONTENT

Supporting Information

The Supporting Information is available free of charge at https://pubs.acs.org/doi/10.1021/acsomega.1c03821.

Phase transition phenomenon of ELPs-MNPs (MP4)

Phase transition phenomenon of ELPs-$(K5V4F)_{40}$ (MP4)

Expression plasmid of ELPs-$(K5V4F)_{40}$, gene sequence of ELPs-$(K5V4F)_{40}$, and protein sequence of ELPs-$(K5V4F)_{40}$ (PDF)

■ AUTHOR INFORMATION

Corresponding Author

Guangya Zhang − *Department of Bioengineering and Biotechnology, College of Chemical Engineering, Huaqiao University, Xiamen 361021 Fujian Province, PR China;* orcid.org/0000-0002-2357-4854; Email: zhgyghh@hqu.edu.cn

Authors

Yanhong Zhou − *Department of Bioengineering and Biotechnology, College of Chemical Engineering, Huaqiao University, Xiamen 361021 Fujian Province, PR China*

Bo Zeng − *Department of Bioengineering and Biotechnology, College of Chemical Engineering, Huaqiao University, Xiamen 361021 Fujian Province, PR China*

Rui Zhou − *Department of Bioengineering and Biotechnology, College of Chemical Engineering, Huaqiao University, Xiamen 361021 Fujian Province, PR China*

Xialan Li − *Department of Bioengineering and Biotechnology, College of Chemical Engineering, Huaqiao University, Xiamen 361021 Fujian Province, PR China*

Complete contact information is available at: https://pubs.acs.org/10.1021/acsomega.1c03821

Notes

The authors declare no competing financial interest.

■ ACKNOWLEDGMENTS

This work was funded by the Natural Science Foundation of Fujian Province of China (2020J01079).

■ REFERENCES

(1) Lisjak, D.; Mertelj, A. Anisotropic magnetic nanoparticles: A Review of Their Properties, Syntheses and Potential Applications. *Prog. Mater. Sci.* **2018**, *95*, 286−328.

(2) Wu, K.; Su, D.; Liu, J.; Saha, R.; Wang, J.-P. Magnetic Nanoparticles in Nanomedicine: a Review of Recent Advances. *Nanotechnology* **2019**, *30*, 502003.

(3) Li, L.; Yang, W.-W.; Xu, D.-G. Stimuli-Responsive Nanoscale Drug Delivery Systems for Cancer Therapy. *J. Drug Target.* **2019**, *27*, 423−433.

(4) Sun, X.; Sun, S. Preparation of Magnetic Nanoparticles for Biomedical Applications. *Methods Mol. Biol.* **2017**, *1570*, 73−89.

(5) Saha, A.; Ben Halima, H.; Saini, A.; Gallardo-Gonzalez, J.; Zine, N.; Viñas, C.; Elaissari, A.; Errachid, A.; Teixidor, F. Magnetic Nanoparticles Fishing for Biomarkers in Artificial Saliva. *Molecules* **2020**, *25*, 3968−3988.

(6) Krishnan, B. P.; Prieto-López, L. O.; Hoefgen, S.; Xue, L.; Wang, S.; Valiante, V.; Cui, J. Thermomagneto-Responsive Smart Biocatalysts for Malonyl-Coenzyme A Synthesis. *ACS Appl. Mater. Interfaces* **2020**, *12*, 20982−20990.

(7) Liu, F.; Shah, D. S.; Gadd, G. M. Role of Protein in Fungal Biomineralization of Copper Carbonate Nanoparticles. *Curr. Biol.* **2021**, *31*, 358−368.

(8) McCausland, H. C.; Komeili, A. Magnetic genes: Studying the genetics of biomineralization in magnetotactic bacteria. *PLoS Genet.* **2020**, *16*, No. e1008499.

(9) Bazylinski, D. A.; Frankel, R. B.; Jannasch, H. W. Anaerobic Magnetite Production by a Marine, Magnetotactic Bacterium. *Nature* **1988**, *334*, 518−519.

(10) Vargas, G.; Cypriano, J.; Correa, T.; Leão, P.; Bazylinski, D.; Abreu, F. Applications of Magnetotactic Bacteria, Magnetosomes and Magnetosome Crystals in Biotechnology and Nanotechnology: Mini-Review. *Molecules* **2018**, *23*, 2438−2462.

(11) Lefèvre, C. T.; Bennet, M.; Landau, L.; Vach, P.; Pignol, D.; Bazylinski, D. A.; Frankel, R. B.; Klumpp, S.; Faivre, D. Diversity of Magneto-Aerotactic Behaviors and Oxygen Sensing Mechanisms in Cultured Magnetotactic Bacteria. *Biophys. J.* **2014**, *107*, 527−538.

(12) Krajina, B. A.; Proctor, A. C.; Schoen, A. P.; Spakowitz, A. J.; Heilshorn, S. C. Biotemplated Synthesis of Inorganic Materials: An Emerging Paradigm for Nanomaterial Synthesis Inspired by Nature. *Prog. Mater. Sci.* **2018**, *91*, 1−23.

(13) Rawlings, A. E.; Somner, L. A.; Fitzpatrick-Milton, M.; Roebuck, T. P.; Gwyn, C.; Liravi, P.; Seville, V.; Neal, T. J.; Mykhaylyk, O. O.; Baldwin, S. A.; Staniland, S. S. Artificial Coiled Coil Biomineralisation Protein for The Synthesis of Magnetic Nanoparticles. *Nat. Commun.* **2019**, *10*, 2873−2881.

(14) Lenders, J. J. M.; Altan, C. L.; Bomans, P. H. H.; Arakaki, A.; Bucak, S.; de With, G.; Sommerdijk, N. A. J. M. A Bioinspired Coprecipitation Method for The Controlled Synthesis of Magnetite Nanoparticles. *Cryst. Growth Des.* **2014**, *14*, 5561−5568.

(15) Roberts, S.; Dzuricky, M.; Chilkoti, A. Elastin-Like Polypeptides as Models of Intrinsically Disordered Proteins. *FEBS Lett.* **2015**, *589*, 2477−2486.

(16) Mullerpatan, A.; Chandra, D.; Kane, E.; Karande, P.; Cramer, S. Purification of Proteins Using Peptide-Elp Based Affinity Precipitation. *J. Biotechnol.* **2020**, *309*, 59−67.

(17) Lin, R.; Wang, S.; Liu, W. Protein-derived Smart Materials for Medical Applications: Elastin-like Polypeptides. *Curr. Pharm. Des.* **2018**, *24*, 3008−3013.

(18) McDaniel, J. R.; Callahan, D. J.; Chilkoti, A. Drug Delivery to Solid Tumors by Elastin-Like Polypeptides. *Adv. Drug Deliv. Rev.* **2010**, *62*, 1456−1467.

(19) Lin, Y.; Jin, W.; Qiu, Y.; Zhang, G. Programmable Stimuli-Responsive Polypeptides for Biomimetic Synthesis of Silica Nanocomposites and Enzyme Self-Immobilization. *Int. J. Biol. Macromol.* **2019**, *134*, 1156−1169.

(20) Yeboah, A.; Cohen, R. I.; Rabolli, C.; Yarmush, M. L.; Berthiaume, F. Elastin-Like Polypeptides: A Strategic Fusion Partner for Biologics. *Biotechnol. Bioeng.* **2016**, *113*, 1617−1627.

(21) Qiu, Y.; Lin, Y.; Zhang, G. Unique Silica Biomimetic Mineralization of Acidic Elastin-Like Polypeptides Without Hydroxyl and Charged Residues. *Int. J. Biol. Macromol.* **2020**, *153*, 224−231.

(22) Reiersen, H.; Clarke, A. R.; Rees, A. R. Short Elastin-Like Peptides Exhibit The Same Temperature-Induced Structural Transitions as Elastin Polymers: Implications for Protein Engineering. *J. Mol. Biol.* **1998**, *283*, 255−264.

(23) Asab, G.; Zereffa, E. A.; Abdo Seghne, T. Synthesis of Silica-Coated Fe3O4 Nanoparticles by Microemulsion Method: Characterization and Evaluation of Antimicrobial Activity. *Int. J. Biomater.* **2020**, *2020*, 4783612.

(24) Kim, W.; Suh, C.-Y.; Cho, S.-W.; Roh, K.-M.; Kwon, H.; Song, K.; Shon, I.-J. A New Method for The Identification and Quantification of Magnetite-Maghemite Mixture Using Conventional X-Ray Diffraction Technique. *Talanta* **2012**, *94*, 348−352.

(25) Schwaminger, S.; Syhr, C.; Berensmeier, S. Controlled Synthesis of Magnetic Iron Oxide Nanoparticles: Magnetite or Maghemite? *Crystals* **2020**, *10*, 214−225.
(26) Jabalera, Y.; Casares Atienza, S.; Fernández-Vivas, A.; Peigneux, A.; Azuaga Fortes, A. I.; Jimenez-Lopez, C. Protein Conservation Method Affects MamC-Mediated Biomineralization of Magnetic Nanoparticles. *Cryst. Growth Des.* **2019**, *19*, 1064−1071.
(27) Rangel-Muñoz, N.; González-Barrios, A. F.; Pradilla, D.; Osma, J. F.; Cruz, J. C. Novel Bionanocompounds: Outer Membrane Protein A and Laccase Co-Immobilized on Magnetite Nanoparticles for Produced Water Treatment. *Nanomaterials* **2020**, *10*, 2278.
(28) Wi, S.; Pancoska, P.; Keiderling, T. A. Predictions of protein secondary structures using factor analysis on Fourier transform infrared spectra: Effect of Fourier self-deconvolution of the amide I and amide II bands. *Biospectroscopy* **1998**, *4*, 93−106.
(29) Bolivar, J. M.; Nidetzky, B. Positively Charged Mini-Protein Zbasic2 As a Highly Efficient Silica Binding Module: Opportunities for Enzyme Immobilization on Unmodified Silica Supports. *Langmuir* **2012**, *28*, 10040−10049.
(30) Tavakoli, Z.; Rasekh, B.; Yazdian, F.; Maghsoudi, A.; Soleimani, M.; Mohammadnejad, J. One-step separation of the recombinant protein by using the amine-functionalized magnetic mesoporous silica nanoparticles; an efficient and facile approach. *Int. J. Biol. Macromol.* **2019**, *135*, 600−608.
(31) Li, T. L.; Wang, Z.; You, H.; Ong, Q.; Varanasi, V. J.; Dong, M.; Lu, B.; Paşca, S. P.; Cui, B. Engineering a Genetically Encoded Magnetic Protein Crystal. *Nano Lett.* **2019**, *19*, 6955−6963.
(32) Lenders, J. J. M.; Zope, H. R.; Yamagishi, A.; Bomans, P. H. H.; Arakaki, A.; Kros, A.; de With, G.; Sommerdijk, N. A. J. M. Bioinspired Magnetite Crystallization Directed by Random Copolypeptides. *Adv. Funct. Mater.* **2015**, *25*, 711−719.
(33) Contreras-Montoya, R.; Jabalera, Y.; Blanco, V.; Cuerva, J. M.; Jimenez-Lopez, C.; Alvarez de Cienfuegos, L. Lysine as Size-Control Additive in a Bioinspired Synthesis of Pure Superparamagnetic Magnetite Nanoparticles. *Cryst. Growth Des.* **2020**, *20*, 533−542.
(34) Singh, R. K.; Kim, T.-H.; Patel, K. D.; Knowles, J. C.; Kim, H.-W. Biocompatible Magnetite Nanoparticles with Varying Silica-Coating Layer for Use in Biomedicine: Physicochemical and Magnetic Properties, and Cellular Compatibility. *J. Biomed. Mater. Res., Part A* **2012**, *100A*, 1734−1742.
(35) Lazzarini, A.; Colaiezzi, R.; Passacantando, M.; D'Orazio, F.; Arrizza, L.; Ferella, F.; Crucianelli, M. Investigation of Physico-Chemical and Catalytic Properties of the Coating Layer of Silica-Coated Iron Oxide Magnetic Nanoparticles. *J. Phys. Chem. Solids* **2021**, *153*, 110003.
(36) Mirabello, G.; Lenders, J. J. M.; Sommerdijk, N. A. J. M. Bioinspired Synthesis of Magnetite Nanoparticles. *Chem. Soc. Rev.* **2016**, *45*, 5085−5106.

https://doi.org/10.1021/acsomega.1c03821
ACS Omega 2021, 6, 27946−27954